

Improved QPSK modem communication performance for acoustic signals using adaptive digital equalizers

Nada Sharis^{1*}

Iraqi Ministry of Education, Vocational Education Department, Najaf, Iraq

*Corresponding author E-mail: nadakadhom@gmail.com

Received Nov. 9, 2024

Revised Dec. 29, 2024

Accepted Feb. 01, 2025

Online Feb. 24, 2025

Abstract

Transmission reliability in voice communications is an important challenge due to various effects such as multipath propagation, rapid channel changes, and Doppler shift. In this study, QPSK modulation is combined with the transmitter channel equalizer in the receiver part as well as in the transmitter, where a unit for suppressing audio interference and distortions is developed to reduce the effects of the transmitter channel on the waves transmitted through it. An in-depth analysis of the improved digital equalizer device is discussed by comparing different results obtained by varying the design parameters. An optimized digital channel equalization unit is selected from the simulation results, which is used to create a multimedia wireless audio communication system. Better BER performance is expected at the minimum signal-to-noise ratio (SNR) required at the detector input.

Keywords: QPSK modulation, Multipath propagation, Adaptive digital equalizer, Acoustic channel, Bit error rate, Signal-to-noise ratio

© The Author 2025.

Published by ARDA.

1. Introduction

Recently, with the advancement of digital communications technologies, MIMO frameworks have become a strong candidate for 5G telecommunications schemes as they are now generally utilized for guaranteed innovation. The increasing number of customers requiring increased data rates has pushed smart and existing partners to go as far as possible by adopting many new developments. Monstrous MIMO is a modern strategy where different radio wires deliver amazing throughput. Moreover, an interesting exhibition was achieved when symmetric redundancy division multiplexing (OFDM) was incorporated into MIMO. Experts have been interested in MIMO-OFDM systems for over a decade. Several research papers [1] have examined waveforms using MIMO structures. However, the MIMO channel evaluation and display issue has been examined by several authors [2-6]. Nevertheless, to the extent that we might actually be aware, there has been as of in the not-so-distant past no review paper that expressly discusses the new examinations in regards to channel evaluation with the implementation of the MIMO-OFDM structures activity. The exception is that there are a few review articles [7] on the MIMO-OFDM structures used especially for the lowered sound correspondence thought, where the correspondence limitations are absolutely one of a kind to those of a long-air correspondence.

As a matter of fact, computerized signal handling as well as direct assessment in hearty MIMO models are likewise the subject of certain examinations [8]. Subsequently, there is a prerequisite for broad review papers that stall the continuous MIMO waveforms, channel evaluation, and change techniques. Thus, the ongoing paper

orders MIMO-OFDM signals, and balancers with channel assessors, have provided a complete outline of the utmost present advantages of MIMO models overall. As well as delineating the paper's coherent construction, Figure 1 portrays a stream graph for the different examination tomahawks which will be talked about in this proposal. The stream outline introduced in above Figure 1 will delineate the construction of the MIMO-OFDM research directions and applications in the computerized correspondence field.

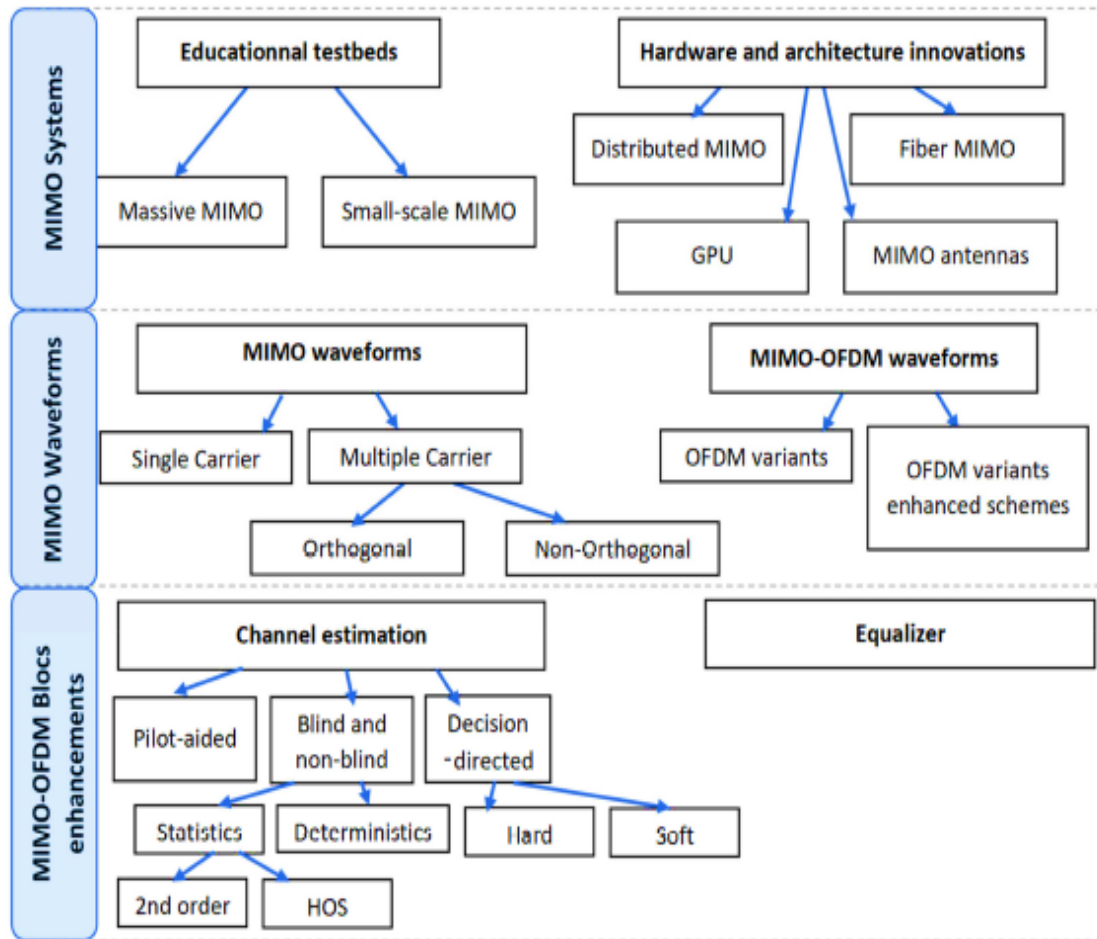


Figure 1. Demonstration of the various research axes utilized for 5G communication systems [8]

The beginning of remote correspondence can be followed back to the late nineteenth hundred years when M.G. Marconi spearheaded the approach involved with laying out the main effective radio connection between a towing boat and a story station. Starting then and into the foreseeable future, far-off correspondence structures have interminably advanced at a shocking rate. Throughout the course of many years, the number of individuals who buy into cell administrations has altogether expanded. Worldwide, the quantity of PDA clients has expanded from two or three thousand toward the start of the twentieth hundred years to roughly 1.5 billion in 2004 [9]. With the ability to give superior grades, and fast information to move between compact gadgets found anyplace on the planet, remote communications is an out-of-the-blue growing fragment of the communications business. It has been the concern of assessment for the clarification that in the 1960s, the extraordinary improvement of distant conversation time was an immediate consequence of the crossroads of different factors.

To start with, there is a developing interest in remote networks. Second, a mind-boggling signal handling and coding calculation can now be carried out in little, low-energy locales because of huge headways in the VISL era. Thirdly, the remote discussion standard of the subsequent time, which incorporates CDMA, GSM, and TDMA, takes into account the low-volume transmission of virtual voice and data. Furthermore, the high-level ghostly effectiveness of the third era of remote communications might provide clients a significantly more predominant assistance [10]. Current remote correspondence frameworks take a stab at high information rates,

reliable communications, extended inclusion, and lower power necessities. MIMO, or numerous information and results, will be viewed as an expected answer for these issues. MIMO innovation further develops correspondence frameworks' unwavering quality and expands their unearthly intensity [11]. Speed is improved and inclusion space is extended through agreeable succession correspondence [12]. The Internet of Things (IoT) is a pristine peculiarity that includes smart remote gadgets flawlessly changing and joining the world. Each part of wellbeing and business is impacted by IoT [13]. The IoT is supposed to incorporate an assortment of remote specialized gadgets [14]. The MIMO-OFDM correspondence model block graph is introduced in Figure 2.

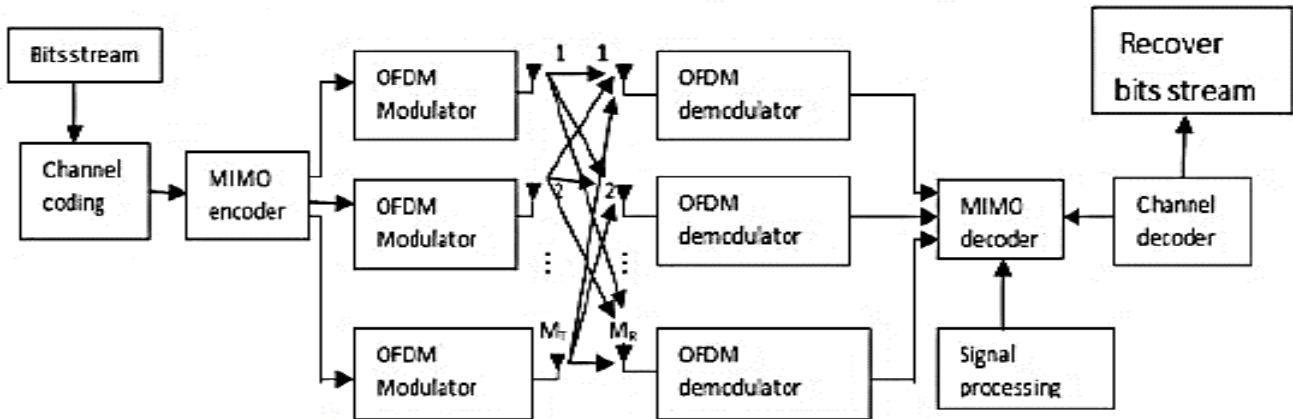


Figure 2. Block MIMO-OFDM communication model block diagram [14]

In reality, there are three central matters that can be utilized to sum up the main pressing concerns with MIMO-OFDM frameworks; 1) channel commotion; Such issue happened when an unwanted arbitrary electromagnetic sign known as added substance weight Gaussian clamor (AWGN) adulterated the sent waveform as it went through the correspondence channel. The communicated sign will be mutilated by the commotion signal, 2) channel obstruction; this issue shows up due to the characteristics of the correspondence channel as well as to external different repeat signals. The impedance issue will also change the properties of the conveyed signal, and 3) synchronization. This issue emerges at whatever point the transmitter and recipient stations' chips switch between different radio waveforms.

Coming up next is an outline of the targets of this proposition that may be gotten from a survey of equivalent past works and accessible writing: 1) Design and recreate a powerful MIMO-OFDM framework to fulfill the cutting-edge computerized correspondence framework; 2) Presenting successful methodologies for lessening and endeavoring to wipe out clamor and obstruction from the got signal and upgrading BER generally; 3) Concerning a reasonable synchronization method to control the exchange time between the transmitter and collector closes; 4) Comparing different plans of MIMO-OFDM models introduced by past examinations and related works. It has been found that a number of MIMO-OFDM survey papers have been explored and introduced. The studies recorded beneath have been distributed to furnish mainstream researchers with a far-reaching investigation of various troublesome issues. In this authentic survey, the most significant and ongoing distributed logical articles and examination talking about the issue of solid advanced communications utilizing MIMO-OFDM numerous info advances will be audited. In 1998, Caire, G., et. al., [7] picked a totally novel multi-pass lattice crossing (MTT) recognition calculation executed along an NVIDIA GPU which performs in basically the same manner as existing calculations, a piece interleave-coded regulation (BICM) was applied. In 2011, CUDA SDK was used to complete the sign-handling blocks of a 2×2 WiMAX MIMO system over an NVIDIA GTX275 GPU, (St Scratch Clara, CA, USA) [8]. The computational show was differentiated and an execution considering TI TMS320C6416 DSP, which shows that the estimation time using a GPU is 3-16 times speedier than the DSP. The total computational time for each single WiMAX outline (of 5 ms length) is 4.346 ms. In 2012, Roger, S., et. al. [9], suggested a circle deciphering calculation based heterogeneous MIMO framework using a GPU-based most extreme probability (ML) signal indicator. In 2014, [10] have proposed the execution of an enormous MIMO assessment with starting outcomes in approval of the framework model.

Likewise, the creators gave a review of without-cell and client-driven enormous MIMO structures. In 2017, Malkowsky, S., et. al. [11], zeroed in on the plan of a design for an enormous MIMO proving ground by considering a few major requests like the casing design, waveform signal plan, as well as the intricacy of the framework. The arrangement was supported inside the Lund School's immense MIMO hardware. The suggested plan maintains up to 100 radio wires and more than 50 FPGAs. In a time division duplex (TDD) (LTE-like TDD) power, an OFDM tweak makes it conceivable to oblige up to 12 clients at the specific recurrence or moment. The tests were completed both inside and outside.

In 2018, [12] have suggested a subsequent equipment proving ground with a base station that has an unearthly productivity of 145.6 bis/s/Hz which could serve 22 clients. Before the base stations, a 128-component patch receiving wire exhibit utilizing a distance of 24.8 m from the transmitter was set up. The time-division duplex (TDD) huge MIMO system works at a carrier repeat of 3.51 GHz with a 256-quadrature amplitude modulation (QAM) plot. An adaptive equalizer (AE) or least mean square error (MMSE) was utilized to ensure hearty data transmission, with an assessment of the direct being done in a cyclic design every 5 milliseconds. In 2018, [13] made an mm-wave MIMO proving ground at the organization of digital signal processing (DSP) at the College of Duisburg-Essen, to work at frequencies under 6 GHz at first. Over the FPGA, DSP, and GPU, it was utilized in a heterogeneous climate. The stage could be reached to some degree through VPN by educational and present-day researchers.

In 2018, [14] sped up the channel assessment in light of least squares (LS) calculation with the uplink OFDM special client MIMO model demodulation utilizing a GPU. The application was completed in a Circle proving ground, to such an extent that different designs of the framework's reaction were assessed corresponding to the radio wires number with the length of the fast Fourier transform (FFT). The analysts accomplish that raising the quantity of receiving wires and the length of the FFT diminishes GPU execution. Thus, they recommended parallelizing the application, utilizing designated calculations, with utilizing a distributed server in ensuing work. In 2018, authors [15] recommended a summarized FDM (GFDM) recipient plan considering index modulation (IM), considering an obscuring direct calculate time. Self-made inter-carrier interference (ICI) and intersymbol interference (ISI) are both wiped out by the planned design. Such issues were achieved by forming channels utilized utilizing GFDM. It uses two-work pivots for multipath correspondence in conditions with quick blurring. The ideal stage turns are achieved by extending the transporter-to-interference ratio (CIR). In 2019, [16] examined the speeding up channel assessment and demodulation of uplink OFDM images for immense scope receiving wire models using the graphics processing unit (GPU). In 2019, [17] led a thorough survey of reconfigurable receiving wires overall for use in 5G applications. They checked out and examined some of the models that were recommended for MIMO and mental radio models. In 2019, Sharief, A.H., et. al., [18], have proposed a fresh out of the plastic new regular discrete wavelet-based MIMO-OFDM system known as MIMO-RDWT-OFDM. The ghostly proficiency of the handset is significantly worked on by the utilization of the recently evolved continuous discrete wavelet change, which does exclude a down-testing step in the deterioration tree.

Furthermore, since it is more impervious to the commotion, it very well might be utilized in AWGN channels like the Rayleigh blurring model. In 2022, [19] proposed one of the first totally supported and commonsense massive MIMO proving grounds with respect to an organized exertion in the midst of the School of Bristol and Lund School, vital for National Instruments (NI). The MIMO-OFDM model is expected for unearthly productivity examination. It has a data transfer capacity of 20 MHz, a testing pace of 30.72 MS/s, and it very well may be used in the recurrence scope of 1.2-6 GHz. Also, it can oblige up to ten clients for each time or recurrence opening and 128 radio wires. A time allotment endures 0.5 milliseconds, uses 1200 subcarriers, and has a phantom proficiency of 145.6 pieces/s/Hz. The rest of the contents of this paper are arranged as follows. The first part of this study, with the help of theoretical principles and mathematical equations, provides an overview of the concept and basic background of the architecture of MIMO-OFDM digital communication technology. In the section on the working method, efficient MIMO-OFDM design schemes are described, which

are proposed and described accurately and in detail. The results of simulation tests are also presented in the third part of this research. Finally, the conclusions section includes evaluating and discussing the results of the study, in addition to future plans.

2. Theory

In this part, the most important theories and basic principles that explain the working principle of MIMO technologies for multiple digital communications will be discussed, which mainly depend on the processes and mechanisms of digital OFDM inclusion. These technologies are considered one of the most important and most modern methods of transmission and reception for fifth-generation digital communications because of the advantages they provide in terms of investing in the transmission channel and the quantity and abundance of information sent through them, in addition to accuracy and efficiency.

2.1. The OFDM technique

In OFDM, the quick bundles of information are segregated towards an assortment of little-speed parcels. Such streams are communicated at the specific span along parts of indistinguishable sub-channels. OFDM isn't just a methodology of organizing, it is a twofold innovation. Sensible imaging would build the OFDM's activities understanding as the beginning in the request is "O", for example symmetrical. Because of such properties, symmetrical recurrence division multiplexing is differentiated along with recurrence division multiplexing. The piece rate thought proposes an essential capability for the recurrence field. Such associated bits change the powerful activity time of one or the other edge. In multicarrier correspondence, the cover would have effective data correspondence transmission capacity assuming the scattering in the midst of the subcarriers is sufficient. The surge of the symmetrical recurrence division multiplexing (OFDM) is a better tweak sum to such an extent that data is deserted toward N adjusted increases of sliding information rate with each flood connected on independent subcarriers. Uninhibitedly talking, it is a kind of multi-transporter worked on a specific method. OFDM has been around for close to 40 years additionally was initially planned through the 1960s as well as 1970s along with examination to limit hindrance in the midst of bordering repeat media [14]. OFDM has been introduced in various circumstances like wideband DSL (ADSL) with upgraded sound/video correspondences.

Besides, OFDM is effectively utilized by a variety of remote organizations because of its information limit against enormous piece rate execution as well as multipath dormancy productivity [15-20]. OFDM has been recommended as a correspondence procedure to help send information quickly along far-off gadgets in multipath circumstances. In the last few years, OFDM has procured toward a standard modified broadband correspondence design, remote or cabled, which is used in executions of, for instance, further developed TV against voice correspondence, far-off foundations with wideband web entrance [16]. In remote cases, appended waveforms succeed different ways to deal with broadcast. At the score rehashed along the total materials, such styles emerge at the getting unit against different engendering slacks continuing in age slack, in the midst of picture impedance (ISI), commotion, with non-systematic stage redirection. For instance, slacked reciprocals of a recorded marker would overlay against the next markers, creating in intersymbol interference (ISI). Through such lines, the speed of sent information is restricted by slacked channel age. OFDM (symmetrical recurrence division multiplexing) frameworks partition the essential band into a few subcarriers. Every one of these subcarriers can be regulated independently. OFDM conspires by and large give many subcarriers isolated by information spaces. At the point when OFDM is taken on, each subcarrier can communicate at a lower image rate, since numerous subcarriers are sent in equal. This works on the proficiency of the strategy with versatile organizations. The OFDM wave arrangement process starts by hindering the images that should be sent after the correspondence interaction. They are considered as information frequencies for the converse quick Fourier change process. This technique makes OFDM images that will be framed later [17-22]. At the point when the IFFT strategy was utilized, a change was accomplished along the otherworldly space to switch it over completely to the time area. In any case, before transmission, an occasional prefix is remembered for OFDM signs to keep away from between image impedance. The discovery part of the OFDM framework should foresee

the fast image change transformation back into the recurrence space. The fundamental distinction among OFDM and OFDMA (symmetrical recurrence division numerous entrance) is that in OFDM, clients are dispensed in light of time as it were. Conversely, clients are dispensed in view of time and recurrence in OFDMA, as shown in Figure 3.

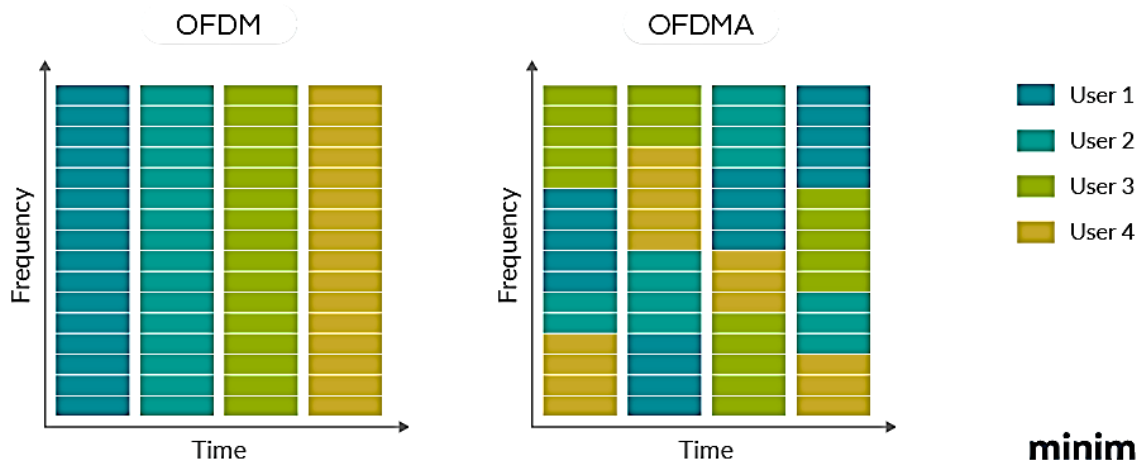


Figure 3. Schematic diagram of the orthogonal communication (a) OFDM, (b) OFDMA [18]

The general model of the OFDM transceiver structure is illustrated in Figure 4 [18-22].

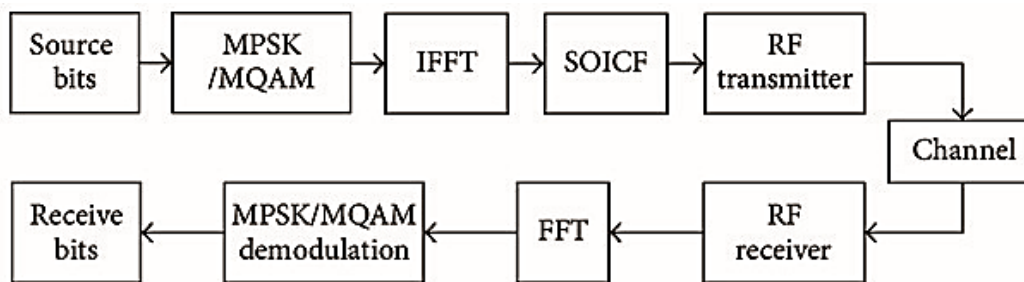


Figure 4. The OFDM transceiver system general structure [22]

2.2. QPSK and QAM OFDM structures

The all-inclusive logical equation of the M-ary PSK sign may be given as [22-30]:

$$S_i(t) = A \cos(\omega_c t + \phi_i(t)) \tag{1}$$

Where; $i=0,1,2,\dots,M-1$

Furthermore;

$$A = \sqrt{\frac{2E}{T_s}} \tag{2}$$

Where ; $\phi_i=0,\pi, m/M$, $m=0,1,2,\dots,M-1$

The limit E is picture energy, T_s is picture time length. The quadrature PSK (QPSK) regulation, $M=4$, and the tweak data signal move the time of the waveform $si t$. The QPSK information move limit capability is 2 pieces/Hz. Similarly as other high level tweak plans, the gathering of stars graph is a useful depiction. In QAM, the glorious body centers are commonly organized in a square grid with identical vertical and level isolating, yet various arrangements are possible (for instance Cross-QAM). Since in mechanized broadcast communications the data are for the most part twofold, the amount of concentrations in the organization is commonly a power of (2, 4, 8 ...). Since QAM is by and large square, a part of these are extraordinary. The most generally perceived structures are 16-QAM, 64-QAM and 256-QAM. By moving to a higher solicitation eminent body, it is practical to convey more pieces per picture. Regardless, on the off chance that the mean

energy of the star gathering is to go on as in the past (through making a sensible assessment), the centers ought to be closer together and are in this manner more powerless to upheaval and other degradation. This results in a higher piece bungle rate subsequently higher-demand QAM might pass on a bigger number of data less reliably than lower-demand QAM, for predictable mean grand body energy. The OFDM transmitter might be executed by utilizing a standard IFFT, however without isolating the yields by N as follows [25-40]:

$$x_k = \sum_{n=1}^{N-1} d_n e^{\frac{j2\pi nk}{N}} \quad (3)$$

$K=0,1,2,\dots,N-1$.

Where d_n is the predefined information picture from bit stream bm and $e^{j2\pi nk/N}$, $n=0,1,\dots,N-1$. Addresses the related symmetrical frequencies of the N sub-transporters. Figure 5a shows an enhanced OFDM transmitter block outline. Note that the S/P is the consecutive to-look-like converter and P/S is the equal constant converter. All baseband exercises are programming based dealing with modules. After P/S, the high-level sign stream is then adhered to the item-adjusted procedure and sent from a distance.

The dealt with beneficiary plan is depicted in Figure 5b. At the collector, the signal is down different over. Expecting that the synchronization cycle has worked out, the mechanized tested signal rk is gone through S/P, FFT dealing with, P/S, and demodulation movement. The last perceived signal d_n of the m th OFDM picture in the added substance white Gaussian upheaval (AWGN) channel is tended to as follows [25-40].

$$\hat{d} = \frac{1}{N} \sum_{k=0}^N r_k e^{\frac{j2\pi nk}{N}} \quad (4)$$

Where, $r_k = r_{k+m} = x_k + w_k$.

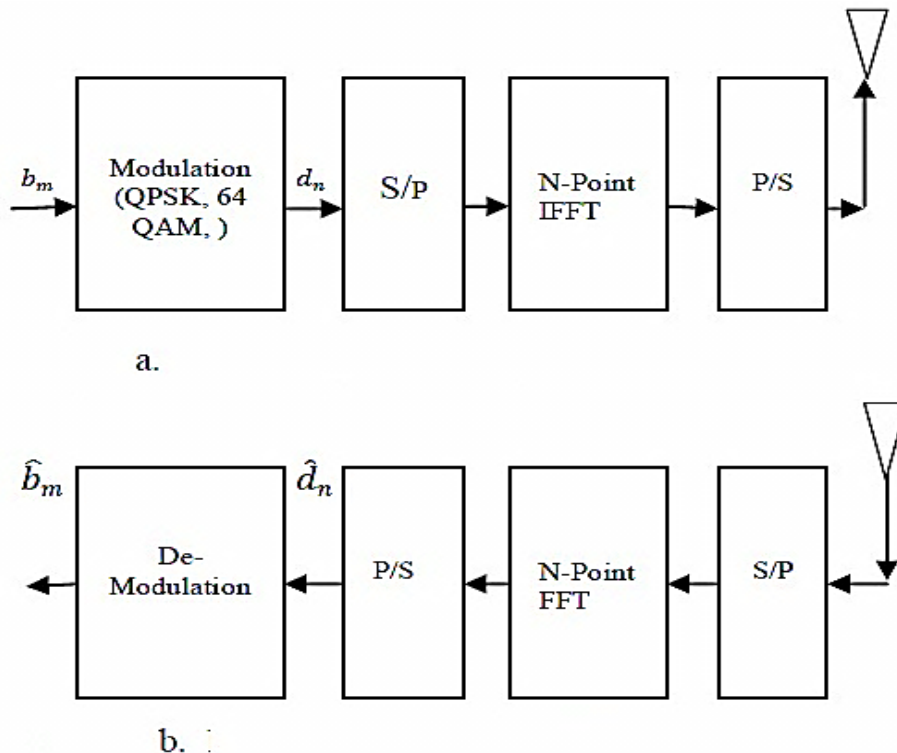


Figure 5. The simplistic OFDM block Diagram, (a) Transmitter, (b) Receiver [30]

3. Methodology

The suggested model of multi-signal correspondence utilizing OFDM's powerful computerized tweak framework has been planned and reenacted with the help of MatLab2020b Simulink tool stash as displayed in Figure 6.

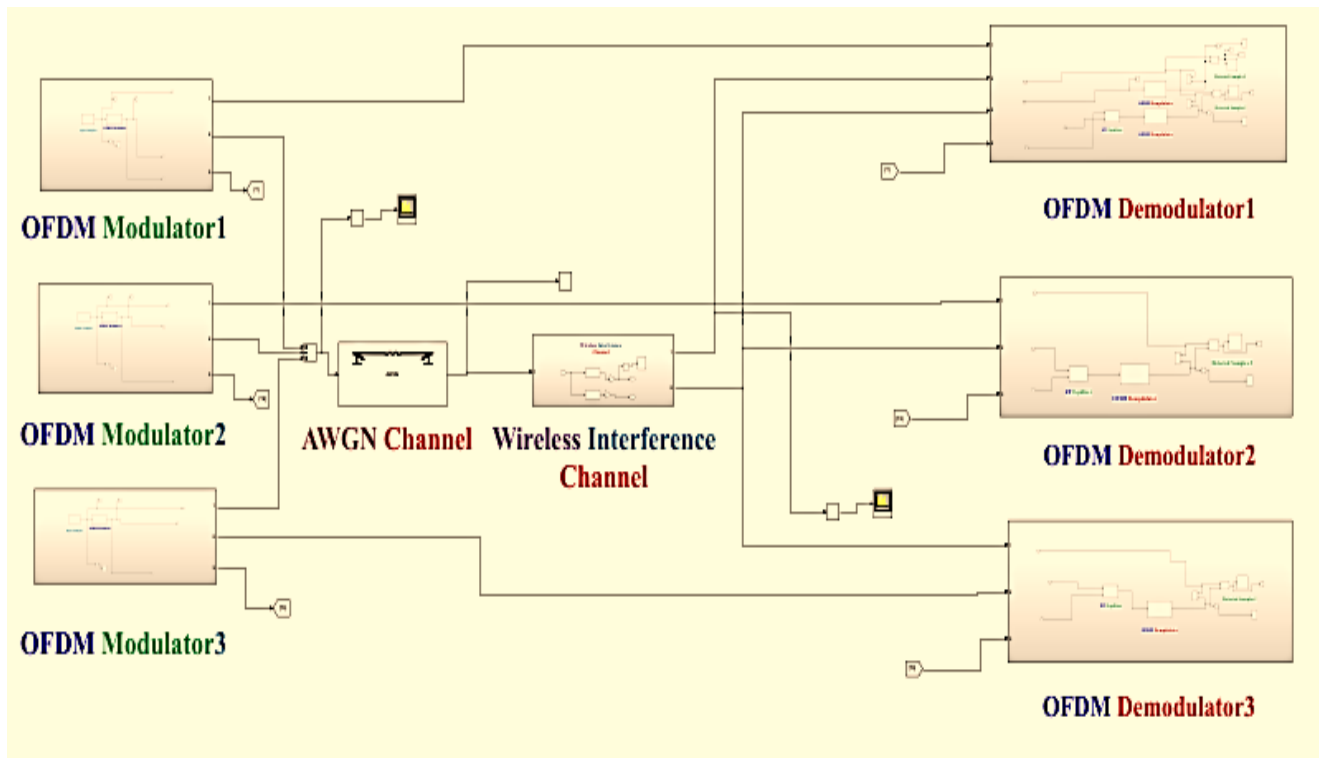


Figure 6. The recommended model of multi-signal correspondence utilizing OFDM's powerful advanced balance framework recreated with the MatLab2020b Simulink tool compartment

By taking into account the recommended model displayed in Figure 6, we could notice the development of the proposed framework model which comprises of three fundamental units which are: the advanced transmitter, communication channel, and the computerized collector units. Every unit will be portrayed with subtleties in the accompanying sections; 1) The digital transmitter unit, 2) The wireless communication channel unit, and 3) the digital receiver unit. Consequently, the essential boundaries and plan specifications used to change the activity of our proposed model execution are recorded in Table 1.

Table 1. The important boundaries and plan specifications used to change the activity of the proposed model execution

| System Type | Sampling Frequency (fs) | Operating Frequency (BW) | Adjustments Details | Design Type | Notes |
|-----------------------------------|-------------------------|-------------------------------|---|--------------------------------|-----------------------------|
| Data Generator Three Users | 2 MHz | (0-1) MHz | Mean=0.1 Variance=0.1 Seed=0.5 | Random Signal Generator | Employ ADC Rb=2 M bps |
| Transmitter System Their Users | 4 GHz | 400 MHz 600 MHz 800 MHz | Bit Rate (Rb)=2 M bps | OFDM/QPSK | Employ IFFT |
| Communication Channel | 4 GHz | (0-2) GHz | SR= 5 dB | AWGN With Interference Channel | Number of bits per symbol=1 |
| Receiver System | 4 GHz | 600 MHz | Integration period (number of samples): 8 | OFDM/QPSK | Employ FFT |

Then, the flowchart of our proposed model committed to executing the multi-signal correspondence utilizing OFDM vigorous advanced regulation framework is introduced as displayed in Figure 7.

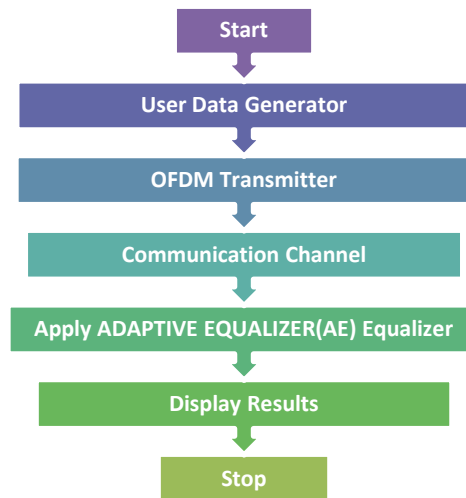
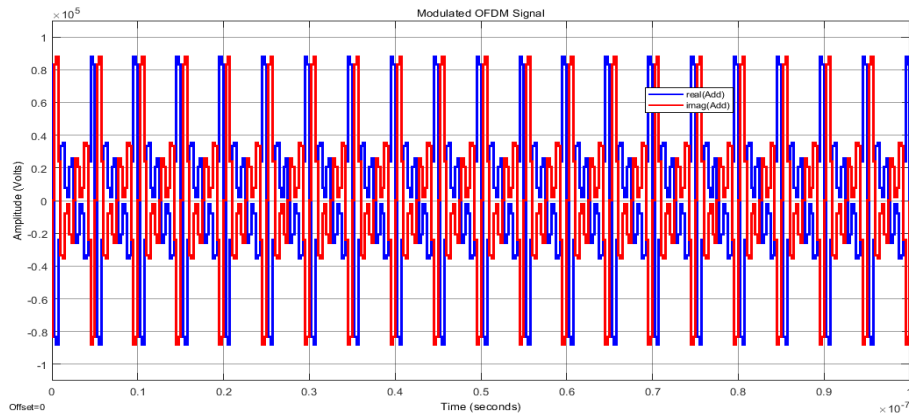


Figure 7. The flowchart of our proposed model dedicated to implementing the multi-signal communication using OFDM robust digital modulation system

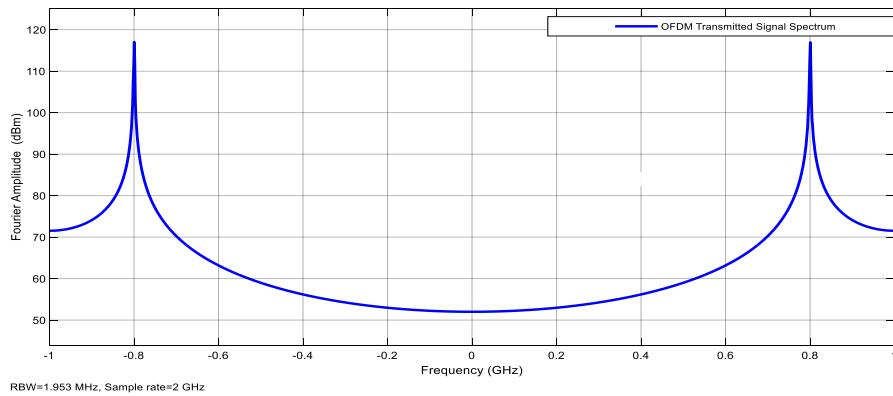
Figure 7, which addresses the stream outline of the functioning instrument of the proposed model for the task, depicts the strategy for executing programs and the progression of signals through the carried-out frameworks. The program starts by setting up the clients' signals and changing their operating qualities and frequencies as per the details expressed in Table 3.1, and afterward setting up the computerized transmission unit to get the clients' signals to incorporate them as per the settled upon component and send them through the reenacted communications channel framework. From that point onward, crafted by the communications channel recreation framework is executed, which likewise works as per the plan particulars expressed in a similar table above to guarantee the execution of the necessities of the task and the postulation. Through the carried out communications channel, arbitrary commotion signals and the impacts of the transmission channel (impedance signals) are added to the sent signal implanted with OFDM innovation to guarantee that the communications direct is reenacted in the most effective way near the sensible down to earth angle. From that point forward, the adaptive equalizer (AE) adjuster module reproduction is called, which works on commotion and impedance handling and attempts to diminish their belongings as indicated by the planned signal-to-clamor power proportion. This is trailed by carrying out a reenactment of the computerized getting and demodulating unit utilizing OFDM computerized demodulating innovation to remove the first signals sent by clients and work out the gathering exactness and location proficiency. At long last, precision computations and confirmation are performed by checking the typical mistake rate and showing these readings to decide the proficiency of the framework's work all in all and to finish the program.

4. Results

The suggested arrangement of innovation for multi-signal correspondence utilizing OFDM's strong computerized adjustment framework has been effectively carried out as per the planned flowchart and changed determinations given in Section III. Where, the thought was carried out utilizing three clients of the communications channel to show the component of multiplexing, where the frameworks intended to execute the stream graph and address all waves and frameworks were reenacted automatically founded on the plan determinations depicted in Section III. The Matlab Simulink climate was utilized, which provides customized framework devices and a productive research facility climate to execute the proposed model and concentrate and look at results. In fact, the accomplished OFDM modulated communicated waveform through the advanced transmitter unit has been shown in Figure 8 in both time and recurrence spectrum areas for client 1 with $f_c=800$ MHz.



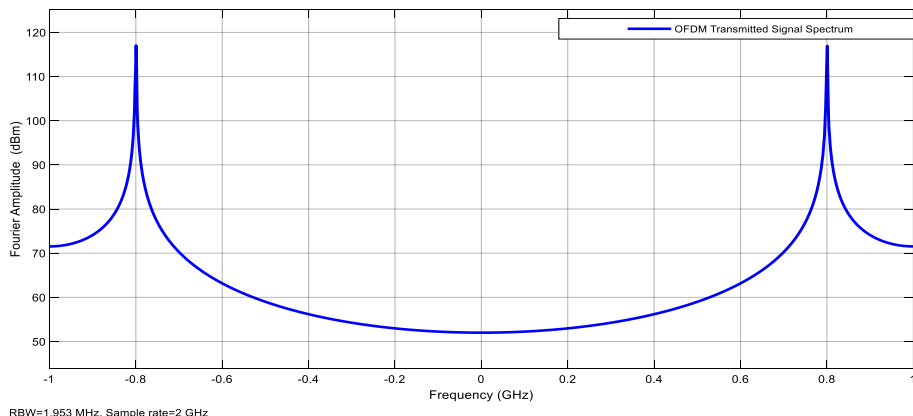
(a)



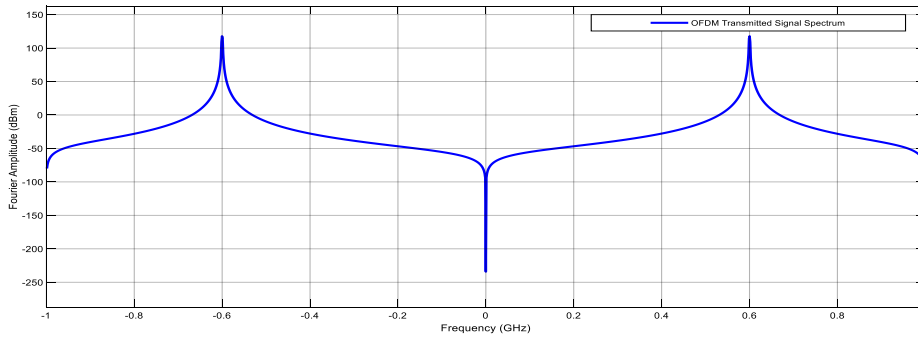
(b)

Figure 8. The accomplished OFDM modulated communicated signal from the computerized transmitter unit for client 1 with $f_c=800$ MHz, (a) In time space, (b) In recurrence spectrum area

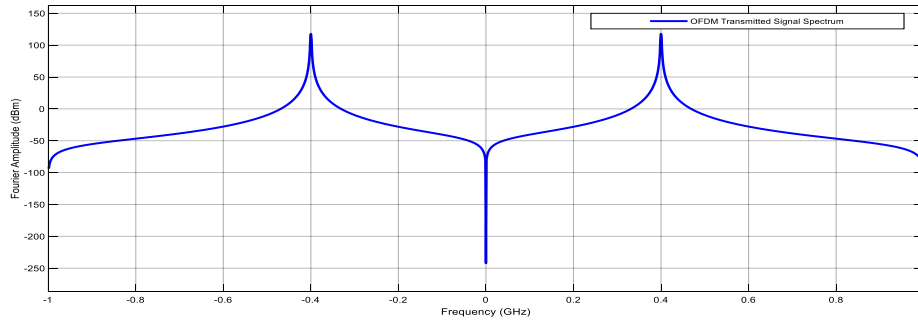
Hence, the modulation waveforms sent from the computerized transmission unit as they might be obviously seen in the time space as displayed in Figure 8a. These signals are sent for the main client or client at a transporter recurrence of $f_c = 800$ MHz, in the wake of being tweaked with OFDM innovation. Moreover, as we could see from Figure 8b that the range or recurrence reaction of such sent with OFDM tweak signals, have unearthly state of similar unique client advanced information however carried on transporter recurrence of $f_c = 800$ MHz. Therefore, these means will be rehashed by the other clients, where we will create transmission signals involving OFDM innovation until the end of the clients with transporter frequencies at $f_c= 400$, and 600 MHz frequencies, so that every client's data is sent on a different transporter recurrence so the transmission succession of the communicated computerized waves covers the recurrence range with the grouping of $f_c= 400$, 600 , and 800 MHz separately. Figure 9 presents the acquired range reaction of every client sent OFDM regulated signal as indicated by the planned grouping of our recommended multi-clients advanced correspondence model.



(a)



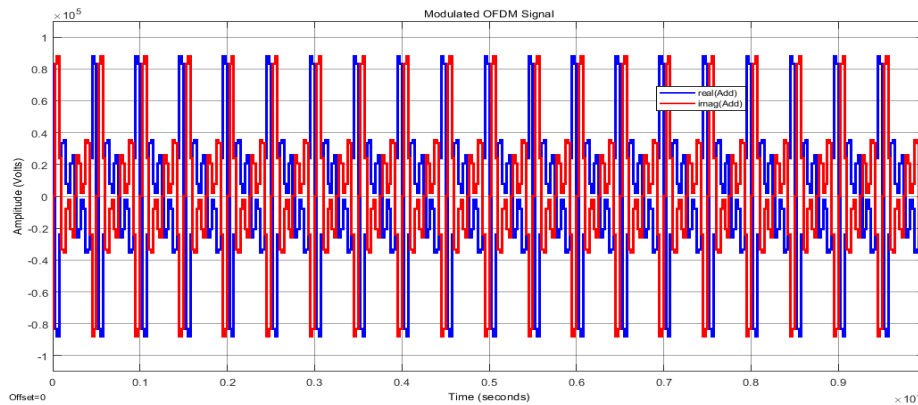
(b)



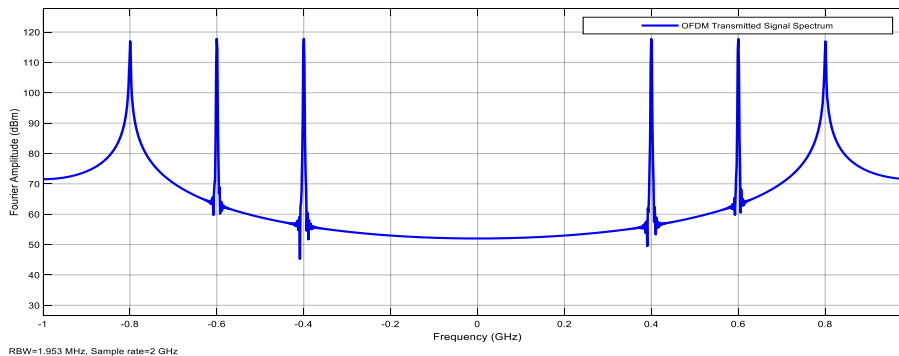
(c)

Figure 9. The got spectrum reaction of each sent OFDM modulated client signal as indicated by the planned succession of our proposed model, (a) $f_C=800$, (b) $f_C=600$, and (c) $f_C=400$ MHz

Then, this multitude of signals will be included to be sent through the reproduced remote correspondence channel. Figure 10 shows the subsequent signals in the wake of adding all the three sent OFDM waveforms before passage to the remote correspondence divert in time and recurrence areas.



(a)



(b)

Figure 10. The subsequent signals in the wake of adding all the three sent OFDM waveforms before entrance to the remote correspondence channel, (a) Period domai, (b) Recurrence space

By alluding to Figure 10, we could notice the assortment of signals shipped off every client, as the trasmitted OFDM signals seem joined as displayed in Figure 10a. Additionally, by taking a gander at the spectrum of these gathered signals, we could see the circulation of the spectra for each communicated client signal, each as indicated by its transporter recurrence. Figure 10b shows that the spectra of the data signals for every client have been conveyed by the grouping of transporter frequencies that were planned by (400, 600, and 800) MHz. Presently, the subsequent joined OFDM sent signals in the wake of going through the AWGN remote correspondence as shown in both time promotion recurrence spaces in Figure 11.

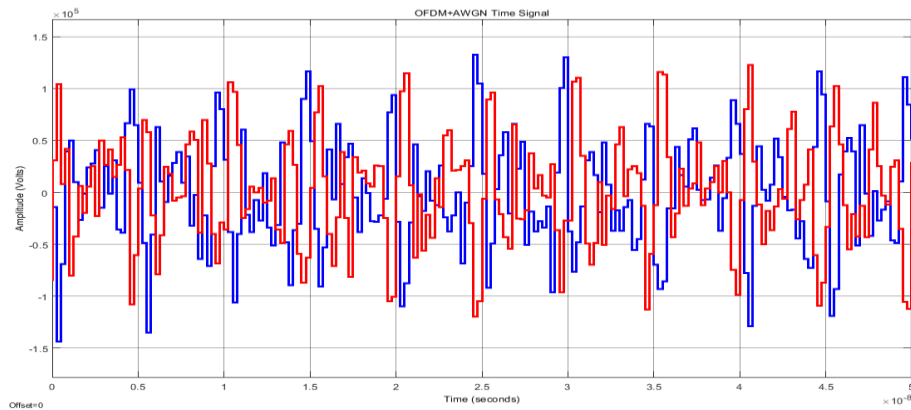
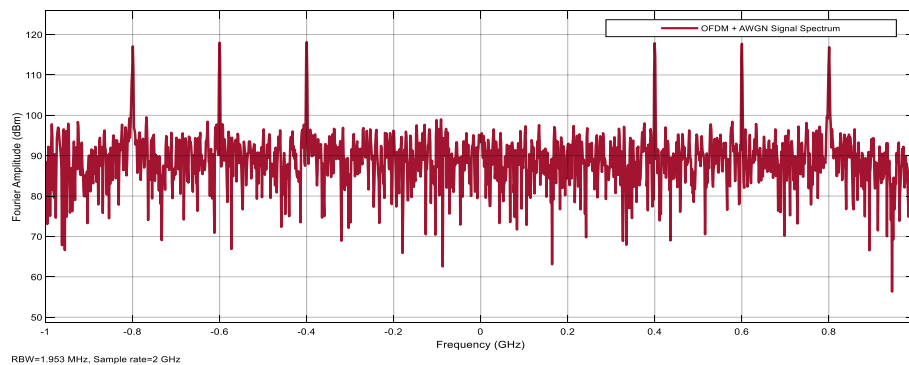


Figure 11. (a) Period domain



(b)

Figure 11. The subsequent consolidated OFDM sent signals in the wake of going through the AWGN remote correspondence channel, (a) Period domain, (b) Recurrence space

As displayed in Figure 11, the consolidated signal of the multi-client communicated wave remembered for the OFDM innovation which has been sent over the AWGN remote communications channel has been presented to get mutilations because of the activity free from the commotion signal examples created by the AWGN communications channel, which impacted the sufficiency and content of the sent OFDM signals sent through it in the time space, as shown on Figure 11a. Likewise, by review the subtleties of the recurrence spectrum wave presented in Figure 11b, we could notice the impact of the commotion wave, the spectra of which seem spread out along the recurrence spectrum of the transmission channel to contort the substance of the carefully implanted OFDM signals sent through the AWGN correspondence channel, with the presence of the upper pieces of the spectra of the communicated waves at every transporter recurrence for every client, while the greater part of the remainder of the spectra content was twisted because of the predominance and impact of the clamor wave spectra. From that point onward, the implanted signals are passed after they leave the AWGN correspondence channel over a reproduced remote impedance channel, which addresses a reenactment of a genuine remote channel that has low-pass channel qualities which influence the sent OFDM waves so their impact shows up as obstruction waves those increment the twisting of the sent OFDM signals through the remote correspondence channel. Figure 12 shows the time and recurrence area states of the subsequent signals in the wake of going through the impedance remote communication channel.

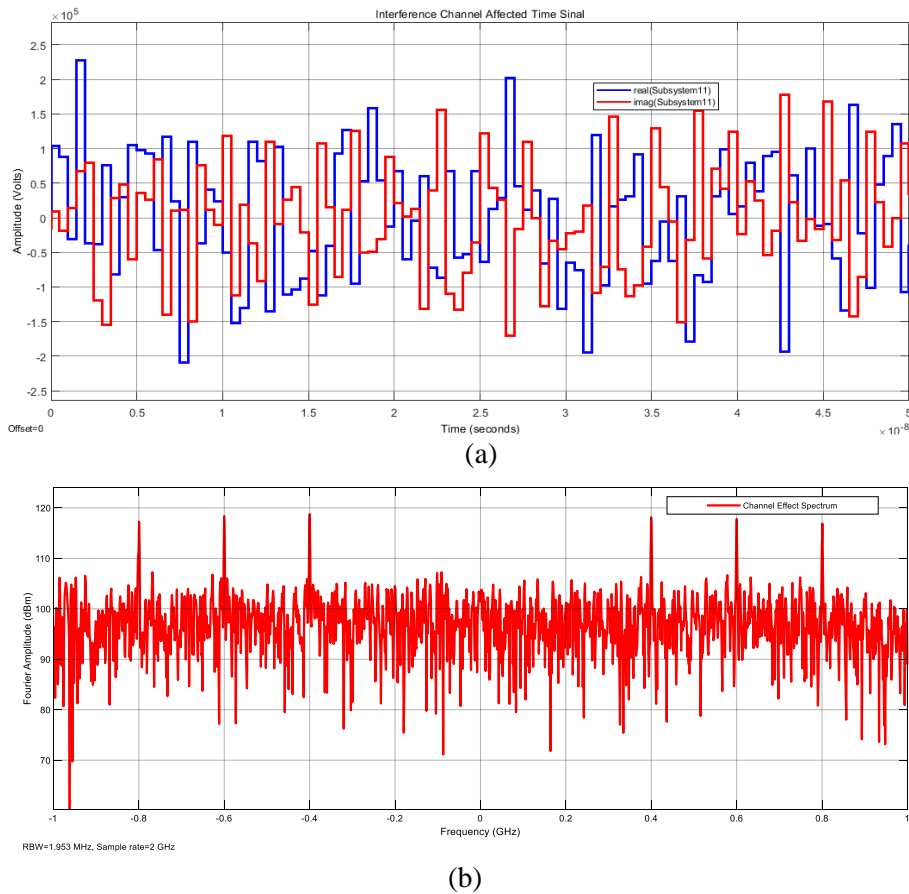


Figure 12. The subsequent signals in the wake of going through the impedance remote correspondence channel, (a) Period space, (b) Recurrence space

Likewise, by auditing Figure 12, we could observe the unexpected impacts of the remote obstruction channel, which increment the bends of the computerized clients joined OFDM modulated signals because of the impact of impedance waves brought about by the qualities of this correspondence channel, as found in Figure 12a for the subsequent signals in the time area. Additionally, by concentrating on the states of the spectrum of the subsequent waves, displayed in Figure 12b, in the wake of going through this channel, we could notice a very clear expansion in the impact of the commotion spectra in the abundance and content, so that the spectra of the included and sent waves scarcely show up at the pinnacles, contingent upon their areas to the frequencies of the transporter waves, while the greater part of the spectra of these waves are lost and twisted with Spectra of clamor and obstruction signals because of the impact of remote communications channel qualities.

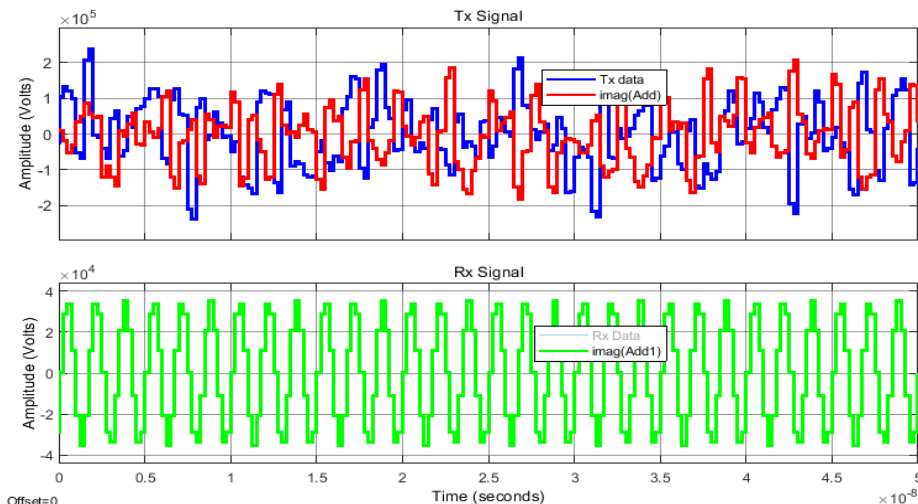


Figure 13(a).

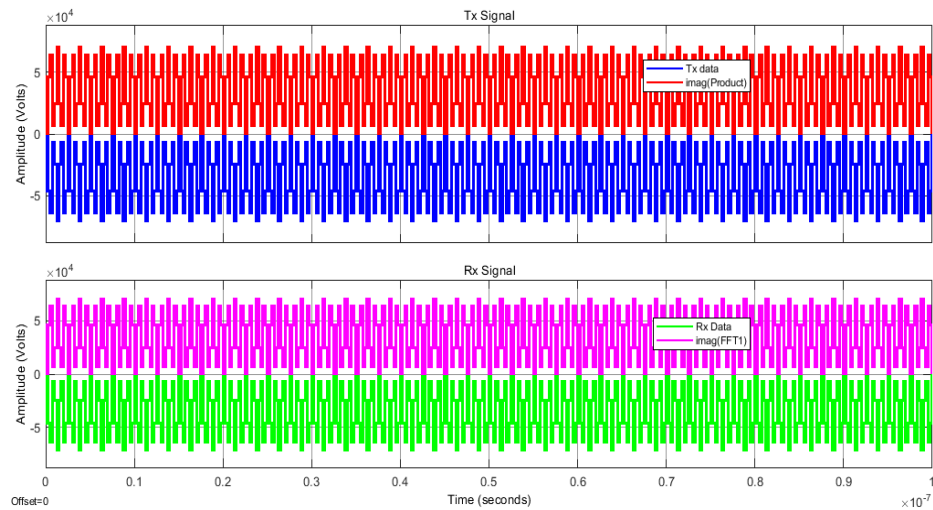


Figure 13(b)

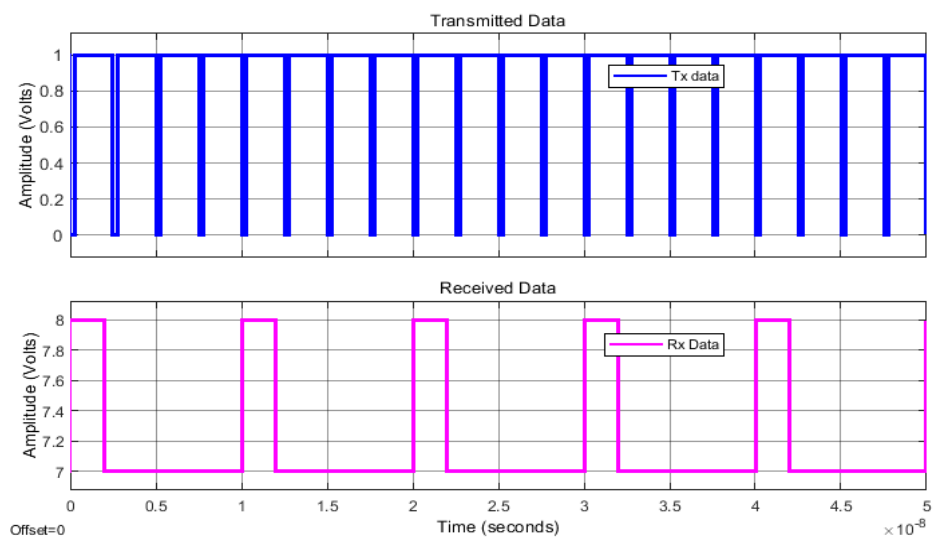


Figure 13(c)

Figure 13. The got signals through the activity of the advanced recipient unit, (a) After blender, (b) After FFT framework, (c) After QPSK demodulator

Alluding to Figure 13, we could see the signals delivered in the time space while the computerized collector is working. Figure 13a shows the source transporter signal created by the recipient oscillator synchronized with the transporter recurrence of the communicated signal (400, 600, and 800) MHz, which show up in the lower half of Figure 13a. In the similar figure we notice in its upper a portion of the subsequent signal in the wake of playing out the blending system, which exhibits the duplications of the obtained signal by its frequencies, which considers demodulation. Likewise, concerning Figure 4.9b, we could perceive the impact of the activity of the FFT framework on the signal in the wake of blending it in with the reference recurrence wave f_c , as this framework works to re-examine the waves and concentrate them from monotonous symmetrical frequencies to create a signal with a solitary transporter recurrence in anticipation of playing out the de-tweak process utilizing the framework QPSK demodulator.

At last, Figure 13c shows the subsequent demodulated signal in the wake of going through the QPSK demodulator framework which shows up at the upper portion of the figure. Likewise, the recognized examples will be accomplished by employing the computerized test and hold framework which will go about as a smooth LPF that will extract the first client information tests from the demodulated waveform as shown in the lower half of Figure 13c. Presently, the recognized client information time tests without utilizing adaptive equalizer (AE) balancer are introduced in Figure 14.

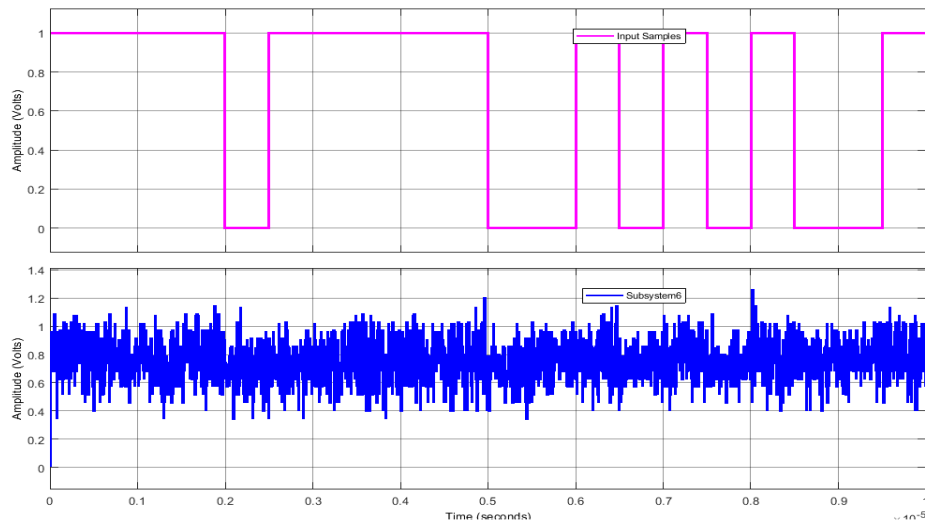


Figure 14 (a)

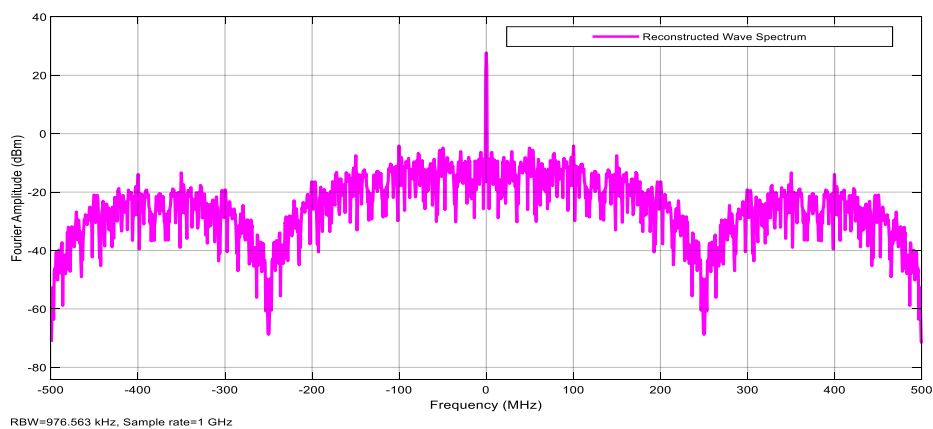


Figure 14 (b)

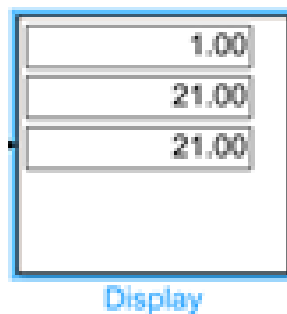


Figure 14 (c)

Figure 14. The recognized client information time tests without utilizing adaptive equalizer (AE) adjuster, (a) Period tests, (b) Spectrum reaction, (c) Mistake rates

Consequently, from checking on Figure 14a, we notice that the signal for client data tests shows up totally twisted because of not connecting with the handling framework addressed by the adaptive equalizer (AE) adjuster before the gathering and de-tweaking process, as displayed in the lower half of the figure. This is because of the twisting of the wave with clamor and impedance waves created inside remote communications channels, which we have recently covered and made sense of. As a matter of fact, we could look at this twisting happening in the client data information signal with the first communicated client data tests introduced in the upper portion of a similar figure. Further, the contortion is hard to miss by noticing the reaction of the recognized client information as displayed in Figure 14b. Since a large portion of the fracture of the spectrum signal was twisted, and the degree of data power was lost because of the impacts of commotion and impedance signal spectra which covered the general spectrum of the computerized signal, consequently losing its highlights. At

last, we could actually look at the got results by looking to the mistake rate revision block showed in Figure 14c, to such an extent that it peruses terrible estimations of the distinguished information tests as contrasted and the first sent information. In addition, presently by including the impact of the adaptive equalizer (AE) balancer framework, the recognized client information time tests are accomplished for the three clients as displayed in Figures 15, 16, and 17, individually.

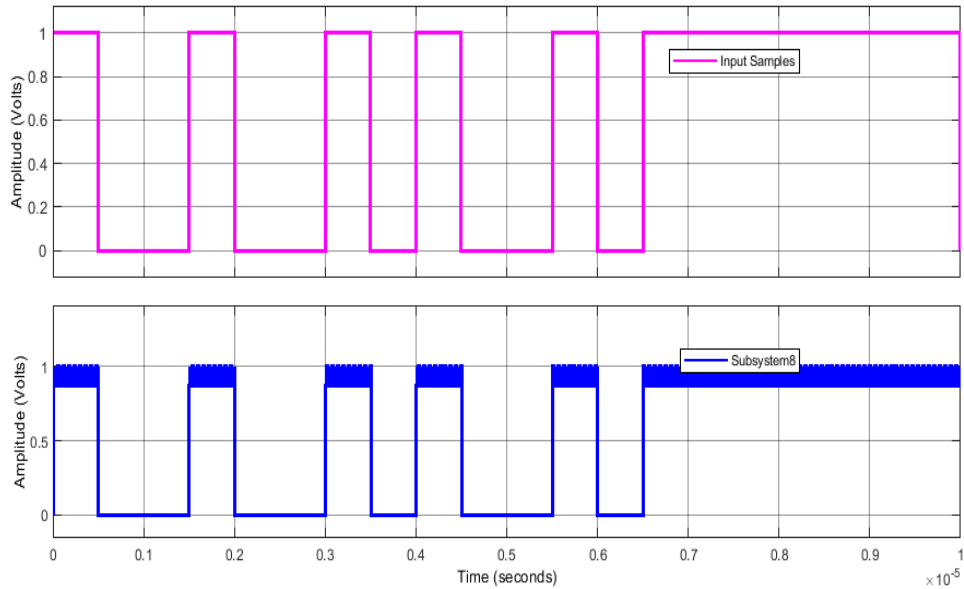


Figure 15 (a)

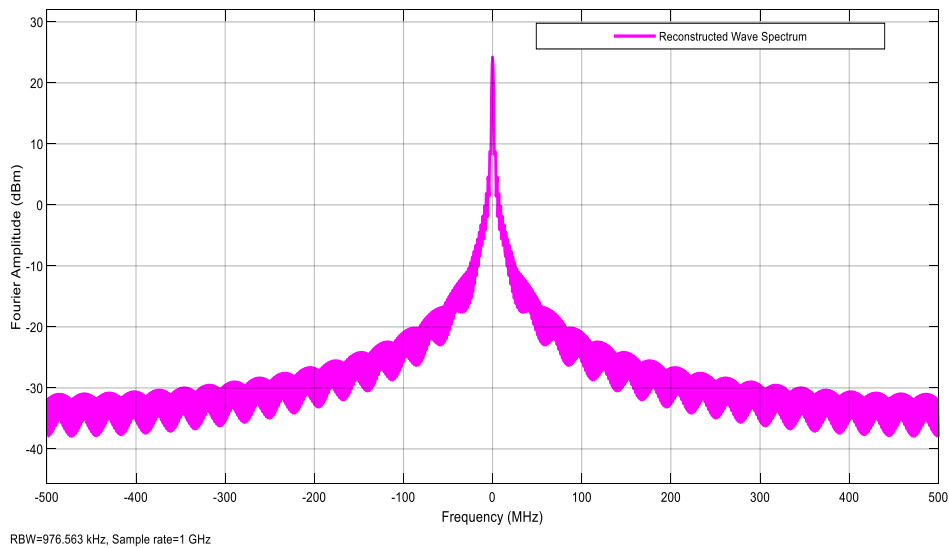


Figure 15 (b)

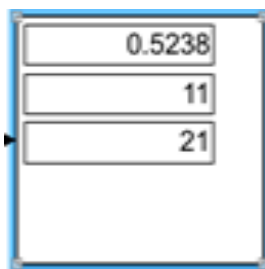


Figure 15 (c)

Figure 15. The recognized client information time tests with including the impact of the adaptive equalizer (AE) balancer framework for the primary client with $f_C=800$ MHz, (a) Period tests, (b) Spectrum reaction, (c) Mistake rates

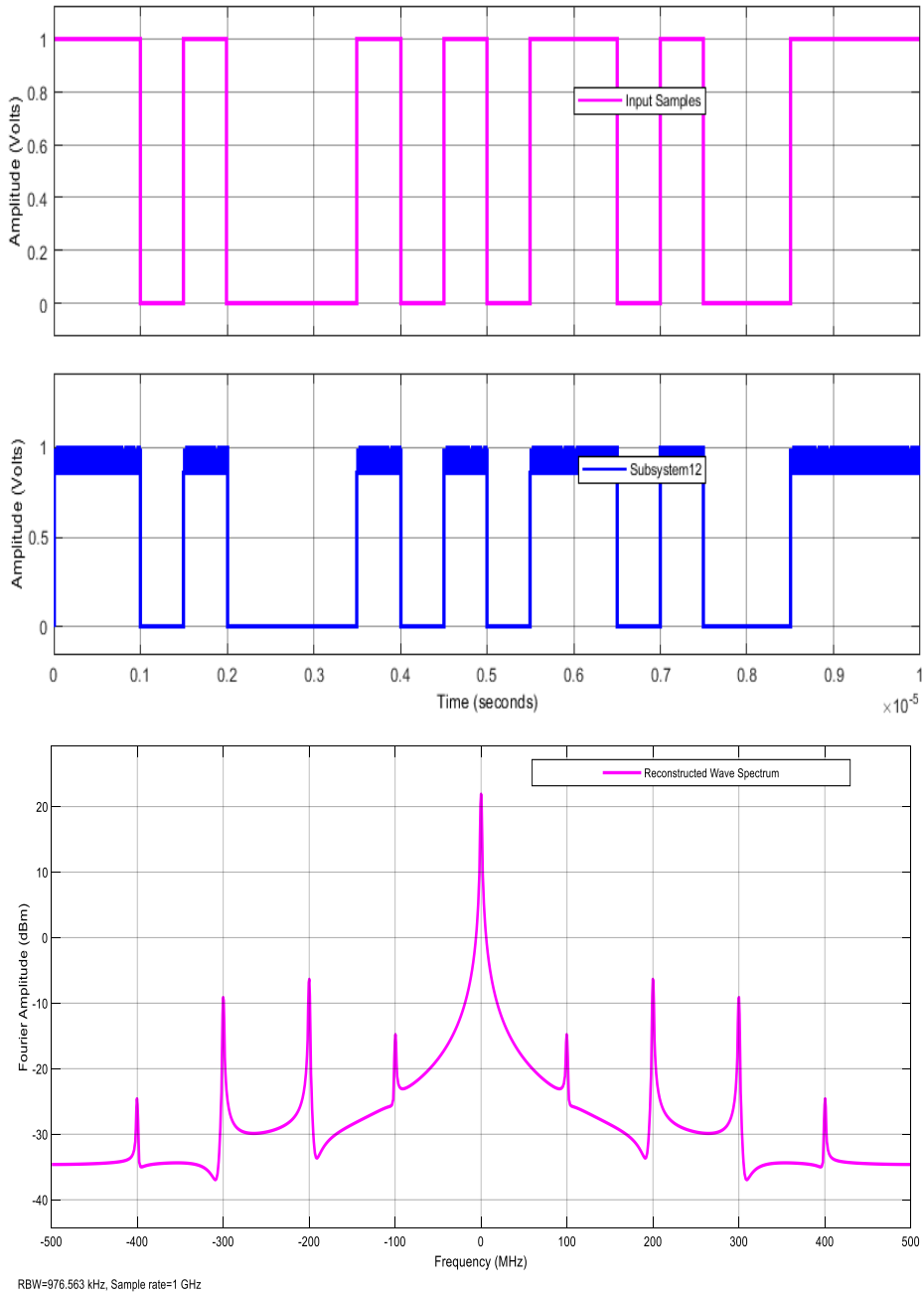


Figure 16 (a)

Figure 16 (b)

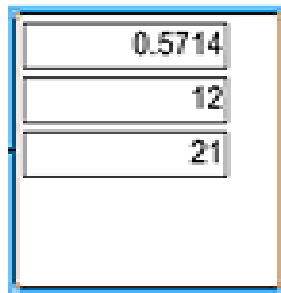


Figure 16 (c)

Figure 16. The distinguished client information time tests with including the impact of the adaptive equalizer (AE) adjuster framework for the primary client with $f_c=600$ MHz, (a) Period tests, (b) Spectrum reaction, (c) Mistake rates

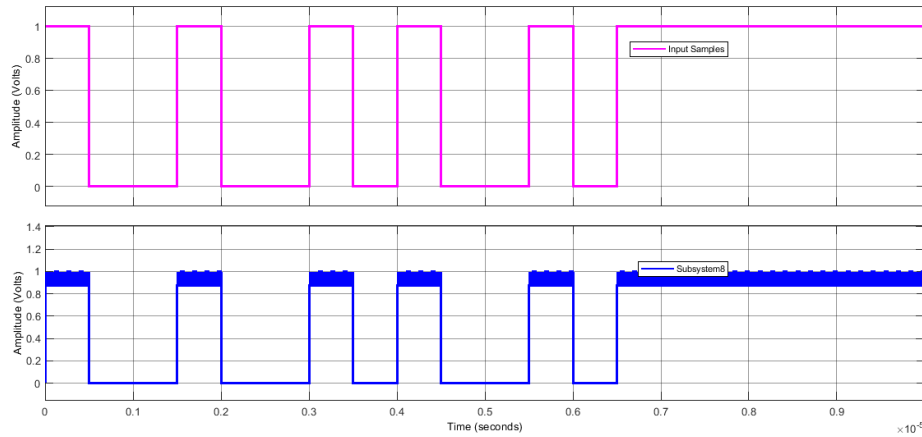


Figure 17 (a)

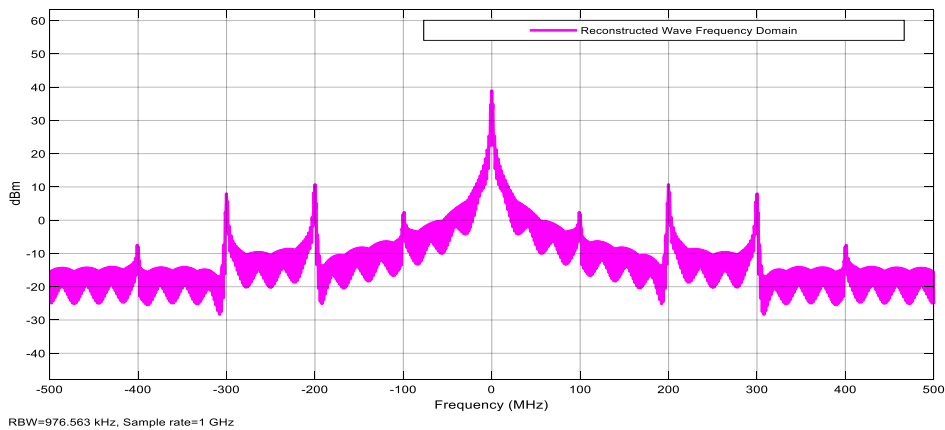


Figure 17 (b)

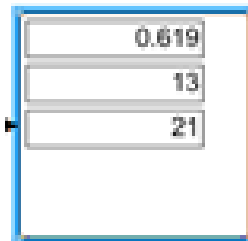


Figure 17 (c)

Figure 17. The identified client information time tests with including the impact of the adaptive equalizer (AE) adjuster framework for the main client with $f_c=400$ MHz, (a) Period tests, (b) Spectrum reaction, (c) Mistake rates

Presently, alluding to Figure 15a, Figure 16a, and Figure 17a, we notice that the signals gotten from the client data tests have been plainly recuperated and give off an impression of being profoundly indistinguishable from the first client data signals sent because of the framework working application. Handling addressed by the adaptive equalizer (AE) balancer before the gathering system, adds to wiping out commotion waves and obstruction and lessening their rate to a base, as displayed in the lower half of the figures above. This is because of the gotten wave disposing of commotion and impedance waves produced inside remote correspondence channels, which we have recently talked about and made sense of. Truth be told, we might look at these outcomes acquired in the client data information signals with the first sent client data tests displayed in the upper portion of similar figures above.

Likewise, by perceiving Figures 15b, 16b, and 17b, we could notice the ghastly reactions of the distinguished information signals for every client information tests which are showed up in agreeable and balanced, and practically liberated from the impacts of clamor spectra and impedance because of the impact of crafted by

adaptive equalizer (AE) adjuster frameworks. Truth be told, there is a distinction in the computerized transmission spectra got for every client, and these distinctions are practically unnoticeable because of the proficiency of the adaptive equalizer (AE) balancer in sifting through the commotion wave spectra and obstruction for each wave the client gets. As in the structures alluded to above. Finally, and alluding to Figures 15c, 16c, and 17c, we could record the got readings of the mistake rates remedies recorded for each recognized client information tests from every client terminal. As a matter of fact, the blunder rate computation framework works to contrast the got information and a deferred duplicate of the sent information and yielding a perusing which addresses the 1) mistake rate, trailed by 2) the quantity of mistakes distinguished and 3) the total number of codes looked at.

Accordingly, the blunder rates remedies of the primary identified client information tests records a mistake pace of 0.524, number of mistakes recognized was 11 mistakes, and absolute number of codes was 21 codes. While the mistake rates revisions of the second distinguished client information tests records a blunder pace of 0.5714, number of blunders identified was 12 mistakes, and number of codes looked at was 21 codes. Likewise, the mistake rates rectifications of the third distinguished client information tests records a blunder pace of 0.619, number of mistakes identified 13 mistakes, and absolute number of codes looked at was 21 codes. Accordingly, in this postulation, a high level model of solid multi-client computerized communications innovation was reenacted utilizing the MATLAB reproduction climate and its supporting devices. The proposed model was intended to reproduce the transmission of three clients over a covering remote Gaussian transmission channel, with the goal that every client was distributed a particular transporter recurrence of (800, 600, and 400) MHz separately. The utilization of the created adaptive equalizer (AE) type adjuster framework was additionally applied, which deals with rearranging the qualities to drive clamor and meddling waves from being stifled and to lessen and take out their consequences for the sent signal inserted through remote communications channels. Through the execution of reenactment projects and frameworks planned as per the principles and controls ready and portrayed ahead of time in the third part on the component for depicting the reasonable and programming angle, the end-product of the venture were acquired, which showed "brilliant" gathering of client data signals utilizing the refreshed adaptive equalizer (AE) balancer framework. The mistake rate was 0.5% with a transmission SNR of 5dB, which made the exactness of the outcomes got exceptionally high, coming to 99.5%. The study can be used as future trends combined with the methodologies reported in [41-52] in different applications.

5. Conclusions

In this research, a strong multi-signal communication model utilizing OFDM vigorous computerized regulation framework is executed and employed utilizing MATLAB reenactment environment and its supporting devices. The suggested model is intended to reproduce the transmission of three clients over a covering remote Gaussian transmission channel, with the goal that every client is relegated a particular transporter recurrence of 800, 600, 400 MHz, separately. The utilization of the created adaptive equalizer (AE) balancer framework has additionally been applied, which deals with switching attributes to drive commotion and impedance waves not to be smothered and to diminish and dispose of their effect on the sent signal installed through remote correspondence channels. Through the execution of recreation projects and frameworks planned as per the norms and controls recently ready and made sense of in the third section on the component for portraying the pragmatic and programming side, the end-product of the task were gotten, which showed "brilliant" gathering of client data signals utilizing the refreshed adaptive equalizer (AE) balancer framework. The blunder rate was 0.5% with a signal-to-commotion proportion (SNR) transmission of 5 dB, which made the precision of the outcomes got exceptionally high, coming to 99.5%.

Declaration of competing interest

The authors declare that they have no known financial or non-financial competing interests in any material discussed in this paper.

Funding information

The authors declare that they have received no funding from any financial organization to conduct this research.

References

- [1] Z. Mokhtari, M. Sabbaghian, and R. Dinis, "A survey on massive MIMO systems in presence of channel and hardware impairments," *Sensors (Basel)*, vol. 19, no. 1, p. 164, 2019.
- [2] O. E. Ijiga, O. O. Ogundile, A. D. Familua, and D. J. J. Versfeld, "Review of channel estimation for candidate waveforms of next generation networks," *Electronics (Basel)*, vol. 8, no. 9, p. 956, 2019.
- [3] F. Wen, H. Wymeersch, B. Peng, W. P. Tay, H. C. So, and D. Yang, "A survey on 5G massive MIMO localization," *Digit. Signal Process.*, vol. 94, pp. 21–28, 2019.
- [4] K. Zheng, L. Zhao, J. Mei, B. Shao, W. Xiang, and L. Hanzo, "Survey of large-scale MIMO systems," *IEEE Commun. Surv. Tutor.*, vol. 17, no. 3, pp. 1738–1760, 2015.
- [5] S. Yang and L. Hanzo, "Fifty years of MIMO detection: The road to large-scale MIMOs," *IEEE Commun. Surv. Tutor.*, vol. 17, no. 4, pp. 1941–1988, 2015.
- [6] J. Zhang, "Review of wideband MIMO channel measurement and modeling for IMT-Advanced systems," *Chin. Sci. Bull.*, vol. 57, no. 19, pp. 2387–2400, 2012.
- [7] G. Caire, G. Taricco, and E. Biglieri, "Bit-interleaved coded modulation," *IEEE Trans. Inf. Theory*, vol. 44, no. 3, pp. 927–946, 1998.
- [8] C. Ahn, J. Kim, J. Ju, J. Choi, B. Choi, and S. Choi, "Implementation of an SDR platform using GPU and its application to a 2×2 MIMO WiMAX system," *Analog. Integr. Circuits Signal Process.*, 2011.
- [9] S. Roger, C. Ramiro, A. Gonzalez, V. Almenar, and A. M. Vidal, "Fully parallel GPU implementation of a fixed-complexity soft-output MIMO detector," *IEEE Trans. Veh. Technol.*, vol. 61, no. 8, pp. 3796–3800, 2012.
- [10] C. Zhang and R. C. Qiu, *Massive MIMO testbed-implementation and initial results in system model validation*. arXiv 2014, 2014.
- [11] S. Malkowsky *et al.*, "The World's First Real-Time Testbed for Massive MIMO: Design, Implementation, and Validation," *IEEE Access*, vol. 5, pp. 9073–9088, 2017.
- [12] W. B. Hasan, P. Harris, A. Doufexi, and M. Beach, "Real-Time Maximum Spectral Efficiency for Massive MIMO and its Limits," *IEEE Access*, vol. 6, pp. 46122–46133, 2018.
- [13] A. Batra, M. Wiemeler, T. Kreul, D. Goehringer, and T. Kaiser, "A Massive MIMO Signal Processing Architecture for GHz to THz Frequencies," in *Proceedings of the 2018 First International Workshop on Mobile Terahertz Systems (IWMTS)*, Duisburg, Germany; Piscataway, NJ, USA: IEEE, 2018, pp. 1–6.
- [14] J. Rodriguez Sanchez, F. Rusek, O. Edfors, M. Sarajlic, and L. Liu, "Decentralized massive MIMO processing exploring Daisy-chain architecture and recursive algorithms," *IEEE Trans. Signal Process.*, vol. 68, pp. 687–700, 2020.
- [15] Y.-K. Chang and F.-B. Ueng, "A novel turbo GFDM-IM receiver for MIMO communications," *Int. J. Electron. Commun.*, vol. 87, pp. 22–32, 2018.
- [16] B. Gokalgandhi, C. Segerholm, N. Paul, and I. Seskar, "Accelerating channel estimation and demodulation of uplink OFDM symbols for large scale antenna systems using GPU," in *2019 International Conference on Computing, Networking and Communications (ICNC)*, 2019.
- [17] M. Kamran Shereen, M. I. Khattak, and G. Witjaksono, "A brief review of frequency, radiation pattern, polarization, and compound reconfigurable antennas for 5G applications," *J. Comput. Electron.*, vol. 18, no. 3, pp. 1065–1102, 2019.
- [18] A. H. Sharief and M. S. Sairam, "Performance analysis of MIMO-RDWT-OFDM system with optimal genetic algorithm," *Int. J. Electron. Commun.*, vol. 111, no. 152912, p. 152912, 2019.

-
- [19] L. Zhao, H. Zhao, K. Zheng, and W. Xiang, *Massive MIMO in 5G Networks: Selected Applications*, 1st ed. Cham, Switzerland: Springer International Publishing, 2018.
- [20] G. Qiao, Z. Babar, L. Ma, and N. Ahmed, "Channel Estimation and Equalization of Underwater Acoustic MIMO-OFDM Systems: A Review Estimation du canal et l'égalisation des systèmes MEMS-MROF acoustiques sous-marins: Une revue," *Can. J. Electr. Comput. Eng.*, vol. 42, pp. 199–208, 2019.
- [21] S. Chen, J. Zhang, J. Zhang, E. Björnson, and B. Ai, "A survey on user-centric cell-free massive MIMO systems," *Digit. Commun. Netw.*, vol. 8, no. 5, pp. 695–719, 2022.
- [22] Ø. Ryan and M. Debbah, "Random Vandermonde Matrices-Part II: Applications," *arXiv [cs.IT]*, 2008.
- [23] J. Vieira *et al.*, "A flexible 100-antenna testbed for Massive MIMO," in *2014 IEEE Globecom Workshops (GC Wkshps)*, 2014.
- [24] S. Malkowsky, L. Liu, V. Owall, and O. Edfors, "Building and operating a real-time massive MIMO testbed — lessons learned," in *2017 51st Asilomar Conference on Signals, Systems, and Computers*, 2017.
- [25] X. Jiang and F. Kaltenberger, "Demo: An LTE compatible massive MIMO testbed based on OpenAirInterface," in *Proceedings of the WSA 2017, 21th International ITG Workshop on Smart Antennas*, Berlin, Germany; Piscataway, NJ, USA: IEEE, 2017, pp. 1–2.
- [26] S. Malkowsky *et al.*, "The world's first real-time testbed for massive MIMO: Design, implementation, and validation," *arXiv [cs.IT]*, 2016.
- [27] A. Batra, M. Wiemeler, T. Kreul, D. Goehringer, and T. Kaiser, "A massive MIMO signal processing architecture for GHz to THz frequencies," in *2018 First International Workshop on Mobile Terahertz Systems (IWMTS)*, 2018.
- [28] C. Zamfirescu, A. Vulpe, S. Halunga, and O. Fratu, "Spatial Multiplexing MIMO 5G-SDR Open Testbed Implementation," in *Lecture Notes of the Institute for Computer Sciences, Social Informatics and Telecommunications Engineering*, Cham: Springer International Publishing, 2019, pp. 197–213.
- [29] C. Ribeiro and A. Gameiro, "A software-defined radio FPGA implementation of OFDM-based PHY transceiver for 5G," *Analog Integr. Circuits Signal Process.*, vol. 91, no. 2, pp. 343–351, 2017.
- [30] H. Zaer Dhaam, M. J. Al Dujaili, M. T. Mezeel, and A. A. Qasim, "Performance of high scalability hybrid system of 10G-TDM-OCDMA-PON based on 2D-SWZCC code," *J. Opt. Commun.*, vol. 44, no. s1, pp. s1121–s1129, 2024.
- [31] H. T. S. Alrikabi, "A Dumbbell Shape Reconfigurable Intelligent Surface for mm-wave 5G Application," *International Journal of Intelligent Engineering & Systems*, no. 6, 2024.
- [32] A. Dujaili and N. H. Abed, "Design a photonic crystal narrowband band pass filter at a wavelength of 1570 nm for fiber optic communication applications," *Wireless Personal Communications*, vol. 131, pp. 877–886, 2023.
- [33] H. T. H. S. ALRikabi, A. Assad, M. J. Al Dujaili, and I. R. N. ALRubei, "Automatic human age estimation from face images using MLP and RBF neural network algorithms in secure communication networks," *Sustainable Engineering and Innovation*, vol. 6, no. 2, pp. 185–198, 2024.
- [34] M. J. Al-Dujaili, "Enhancement of the Fifth Generation of Wireless Communication by Using a Search Optimization Algorithm," *International Journal of Online & Biomedical Engineering*, no. 11, 2023.
- [35] N. H. Abed, M. J. AL-Dujaili, and S. A. Abbas, "Proposed an efficient multilevel dynamic bandwidth allocation (M-DBA) scheme for FiWi networks," *Opt. Quantum Electron.*, vol. 54, no. 10, 2022.
- [36] G. A. Al-Rubaye, H. T. S. Alrikabi, and H. T. Hazim, "Optimization of capacity in non-Gaussian noise models with and without fading channels for sustainable communication systems," *Heritage and Sustainable Development*, vol. 5, pp. 239–252, 2023.
- [37] H. Alrikabi, "Face patterns analysis and recognition system based on Quantum Neural Network QNN," *Int. J. Interac. Mob. Tech.*, vol. 16, no. 8, pp. 35–48, 2022.
-

- [38] A. Y. Sahib, A. Assad, O. M. Mohammed, and H. T. H. S. ALRikabi, "Employing topology optimization method to create optimum telecommunication tower design structure," *Sustainable Engineering and Innovation*, vol. 6, no. 2, pp. 261–274, 2024.
- [39] A. M. Al-awadi and M. J. Al-dujaili, "Simulation of LTE-TDD in the HAPS channel," *Int. J. Electr. Comput. Eng. (IJECE)*, vol. 10, no. 3, p. 3152, 2020.
- [40] B. K. Al-Shammari, "Design of a High Gain Yagi-Uda Antenna Array for VHF-Band Radar Applications. Engineering," *Technology & Applied Science Research*, vol. 14, no. 5, pp. 17188–17195, 2024.
- [41] Y. S. Mezaal and S. F. Abdulkareem, "New microstrip antenna based on quasi-fractal geometry for recent wireless systems," in *2018 26th Signal Processing and Communications Applications Conference (SIU)*, 2018.
- [42] S. Rashed and C. Ozcan, "A Comprehensive Review of Machine and Deep Learning Approaches for Cyber Security Phishing Email Detection," *Al-Iraqia Journal for Scientific Engineering Research*, vol. 3, no. 3, pp. 1–12, 2024.
- [43] M. S. Shareef *et al.*, "Cloud of Things and fog computing in Iraq: Potential applications and sustainability," *Heritage and Sustainable Development*, vol. 5, no. 2, pp. 339–350, 2023.
- [44] H. G. Alsaffar and E. Erçelebi, "Design and Implementation of the IoT Surveillance System using Electronic Appliances with Raspberry Pi," *Al-Iraqia Journal for Scientific Engineering Research*, vol. 3, no. 3, pp. 71–79, 2024.
- [45] Y. S. Mezaal and S. F. Abdulkareem, "Affine cipher cryptanalysis using genetic algorithms," *JP J. Algebra Number Theory Appl.*, vol. 39, no. 5, pp. 785–802, 2017.
- [46] A. Jasim, H. Layth Rafea Hazim, and O. Alwindawi, "Optimizing Prediction of Cardiac Conditions Using Hyper-Adaboost-Integrated Machine Learning Models," *Al-Iraqia Journal for Scientific Engineering Research*, vol. 3, no. 3, pp. 13–24, 2024.
- [47] Y. S. Mezaal, H. T. Eyyuboglu, and J. K. Ali, "Wide Bandpass and Narrow Bandstop Microstrip Filters based on Hilbert fractal geometry: design and simulation results," *PLoS One*, vol. 9, no. 12, p. e115412, 2014.
- [48] A. J. Kadhim and T. S. Atia, "Strengthening Security and Confidentiality in E-Health Systems through Quantum Encryption of Healthcare," *Al-Iraqia Journal for Scientific Engineering Research*, vol. 2, no. 3, pp. 9–21, 2023.
- [49] Y. S. Mezaal and A. S. Al-Zayed, "Design of microstrip bandpass filters based on stair-step patch resonator," *Int. J. Electron.*, vol. 106, no. 3, pp. 477–490, 2019.
- [50] I. Issa, A. Neamah, and F. M. Abdul Razzaq Altahir, "Choosing PSO under Different Overloads to Provide Best Power Flow for IEEE-57 Bus," *Al-Iraqia Journal for Scientific Engineering Research*, vol. 2, no. 3, pp. 64–73, 2023.
- [51] S. A. Abdulameer *et al.*, "Cyber Security Readiness in Iraq: Role of the Human Rights Activists," *International Journal of Cyber Criminology*, vol. 16, no. 2, pp. 1–14, 2022.
- [52] R. A. Jasem, "The Effectiveness of the Mutual Coupling Model, Coupled Voltage to Uncoupled Currents, in Receiving Antenna Arrays," *Al-Iraqia Journal for Scientific Engineering Research*, vol. 3, no. 2, pp. 1–9, 2024.